DOI:
10.1177/0022034517724145

Document Version
Peer reviewed version

Vax1 plays an indirect role in the aetiology of murine cleft palate

Finn Geoghegan [1, 2], Guilherme M. Xavier [1, 2], Anahid A. Birjandi [1], Maisa Seppala [1, 2], Martyn T. Cobourne [1, 2] *

1 Centre for Craniofacial Development and Regeneration

2 Department of Orthodontics

King's College London Dental Institute

Floor 27, Guy's Hospital

London SE1 9RT, UK

* Author for correspondence Martyn T. Cobourne

Tel: 00442071888028

Fax: 00442071881674

martyn.cobourne@kcl.ac.uk

Running title: Vax1 in cleft palate

Key words: forebrain, lobar holoprosencephaly, cleft lip/palate, sonic hedgehog, facial development

Abstract word count: 281

Word count: 3098

References: 38

Figures/Tables 5

Abstract

Cleft lip with or without palate (CLP) or isolated cleft palate (CP) are common human developmental malformations with a complex aetiology that reflects a failure of normal facial development. *VAX1* encodes a homeobox-containing transcription factor identified as a candidate gene for CLP in human populations, with targeted deletion in mice associated with multiple anomalies, including disruption of the visual apparatus and basal forebrain, lobar holoprosencephaly and CP. We have investigated *Vax1* function during murine palatogenesis but find no evidence for a direct role in this process. *Vax1* is not expressed in the developing palate and mutant palatal shelves elevate above the tongue, demonstrating morphology and proliferation indices indistinguishable from wild type. However, mutant mice did have a large midline cavity originating from the embryonic forebrain situated beneath the floor of the hypothalamus and extending through the nasal cavity to expand this region and prevent approximation of the palatal shelves. Interestingly, despite strong expression of *Vax1* in ectoderm of the medial nasal processes, the upper lip remained intact in mutant mice. We found further evidence of disrupted craniofacial morphology in *Vax1* mutants, including truncation of the midface associated with reduced cell proliferation in forebrain neuroectoderm and frontonasal mesenchyme. Sonic hedgehog (Shh) signal transduction was downregulated in the mutant forebrain consistent with a role for Vax1 in mediating transduction of this pathway. However, *Shh* was also reduced in this region, suggestive of an *Shh*-*Vax1* feedback loop during early development of the forebrain and a likely mechanism for the underlying lobar HPE. Despite significant associations between *VAX1* and human forms of CLP we find no evidence of a direct role for this transcription factor in development of this region in a mutant mouse model.

Introduction

Cleft lip with or without the palate (CLP) or isolated clefts of the palate (CP) are relatively common human congenital malformations seen with a prevalence ranging from 1:500-2000 live births, depending upon racial background. The aetiological basis of these disorders is complex but reflects a failure of normal facial development mediated through genetic and environmental factors (Dixon et al. 2011). A number of independent studies have found associations between the homeobox gene *VAX1* and CLP in human populations (Butali et al. 2013; de Aquino et al. 2013; de Araujo et al. 2016; Gowans et al. 2016; Peng et al. 2016; Slavotinek et al. 2012; Wang et al. 2016; Wen and Lu 2016; Zawislak et al. 2014) and Vax genes act downstream of Sonic hedgehog (Shh) (Hallonet et al. 1999; Kim and Lemke 2006; Take-uchi et al. 2003; Zhao et al. 2010) and as both Fgf and Wnt antagonists in a number of developmental contexts (Bharti et al. 2011; Vacik et al. 2011). *Vax1* is first expressed in the early central nervous system (CNS) (Bertuzzi et al. 1999; Hallonet et al. 1998; Taglialatela et al. 2004) and targeted disruption in mice produces multiple defects in the visual apparatus, including coloboma and absence of the optic chiasma, accompanying growth defects in the medioventral CNS, altered axonal guidance and duplication of the pituitary gland (Bertuzzi et al. 1999; Bharti et al. 2011; Hallonet et al. 1999; Taglialatela et al. 2004). Significantly, *Vax1* mutant mice also have lobar holoprosencephaly (HPE) and CP, although the molecular basis of these defects has not been investigated (Bertuzzi et al. 1999; Hallonet et al. 1999).

HPE is a heterogeneous and complex developmental anomaly associated with incomplete division of the embryonic forebrain and classified as alobar, semilobar or lobar, depending upon the amount of cleavage within the telencephalon. A key feature of HPE is aberrant facial development, which can manifest as frank cyclopia or in association with other facial defects, including hypotelorism, single nostril, single median maxillary central incisor (SMMCI) and CLP (Geng and Oliver 2009). HPE has marked clinical variation, with notoriously poor genotypic-phenotypic correlation and wide-ranging intra-familial variability in humans (Ming and Muenke 2002). Moreover, increasing evidence from mouse models

has demonstrated the significance of multiple genetic and environmental factors that can influence phenotype (Heyne et al. 2016; Hong and Krauss 2012).

Here we describe in detail the craniofacial defects associated with loss of *Vax1* in the mouse and further investigate the role of Vax1 during palatogenesis. *Vax1* was expressed in ectoderm of the medial nasal processes within the developing facial region, but transcripts were not identifiable in the secondary palate. Although, loss of *Vax1* is associated with a fully penetrant CP, the upper lip remains intact in mutant mice. We provide evidence to suggest that CP occurs secondary to disruption within the CNS rather than a direct requirement for *Vax1* during palatogenesis. We further identify reduced Shh signal transduction in the early ventral forebrain and reduced levels of proliferation in neuroectoderm of this region in mutant mice. Interestingly, loss of *Vax1* in a background of reduced Shh activity through generation of *Vax1; Gas1* compound mutant mice did not worsen the cleft phenotype, although the SMMCI seen in association with loss of single alleles reverted to complete incisor agenesis in the compound mutants.

Materials and Methods

Generation of *Vax1* and *Gas1* single and compound mutant mice

All procedures were carried out in accordance with the UK Animals (Scientific Procedures) Act (1986) and subject to the approved protocols at King's College London. This study conforms with ARRIVE guidelines. *Vax1* and *Gas1* mice were housed in a Biological Services Unit, generated and maintained on a 129sv/C57BL6 background and genotyped as previously described (Hallonet et al. 1999; Lee et al. 2001). For *Vax1; Gas1* mice both mutant alleles contain a LacZ, therefore genotyping involving two reactions. For the first, the forward primer was constructed to align against the promoter region of *Gas1* [CCGGAGAGTGGAGAAAGGAG]; the reverse primer aligned against the LacZ cassette [CCCCTGAGCATGATCTTCCA] to produce a 392-bp PCR product. For the second, a 350-bp fragment of the wild type (WT) *Gas1* allele deleted in the mutant was amplified using the forward primer [ATCTCGGCGCTTATCCAGCTCAAC] and reverse primer

CATCGCACACGCAGTCGTTGAGCA. Timed-matings were set up such that noon of the day on which vaginal plugs were detected was considered embryonic day (E) 0.5. Pregnant females were euthanized with cervical dislocation. For all experiments, a minimum number of 3 WT and 3 mutant mice were compared.

Histology, skeletal analysis and in situ hybridization

Histological analysis, differential staining of bone and cartilage, radioactive and digoxigenin-section *in situ* hybridisation was conducted as previously described (Seppala et al. 2007); (Oommen et al. 2012).

Proliferation, apoptosis and craniofacial dimensional assays

Bromodeoxyuridine (BrdU) labeling for cell proliferation assays was carried out on histological sections using a Zymed BrdU Labeling and Detection Kit (Invitrogen) according to manufacturer instructions. Mouse embryos were labelled with BrdU via intra-peritoneal injection into pregnant females (5mg/100g body-weight) 2 hours prior to sacrifice. Embryos were fixed in 4% PFA at 4°C overnight, dehydrated in ethanol, embedded in paraffin wax, and sectioned at 7μm. The percentage BrdU-positive cells was calculated.

Immunohistochemical detection of apoptotic cell death was carried out on histological sections using Terminal deoxynucleotidyl transferase-mediated deoxyUridine triPhosphate Nick End Labeling (TUNEL). TUNEL was carried out using an APOPTag® Plus Fluorescein In Situ Apoptosis Detection Kit (Chemicon) according to manufacturer instructions.

Craniofacial dimensions were measured on histological sections using lines constructed from specific anatomical points (Schambra, 2008). All cell counting and linear measurment was conducted by one researcher blinded to experimental group on two separate occasions one week apart and the mean value calculated.

qRT-PCR analysis

qRT-PCR analysis of *Shh*, *Ptch1* and *Nkx2.1* expression was performed on E10.5 WT and *Vax1*$^{-/-}$ embryo heads. Tissue was carefully dissected from the ventral forebrain and facial area and immediately transferred into Trizol. cDNA was synthesized from total RNA and qPCR performed using SYBR® Green PCR Master Mix in an ABI Prism 7900 HT cycler (Applied Biosystems). A standard curve method of quantitation was used to calculate expression of target genes relative to the house keeping gene *β-Actin*. Four serial dilutions of cDNA (1:4) were made for the calibration curve and trend-lines were drawn using Ct values versus log of dilutions for each target gene and *β-Actin* run in triplicate with a correlation coefficient (R^2>0.99). Relative expressions were calculated using line equations derived from calibration curves and obtaining ratios of target gene to *β-Actin*. For each gene, experiments were run at least three times using cDNA obtained from three independent RNA purifications. Data was analysed as previously described (Livak and Schmittgen 2001).

Results

***Vax1* mutant mice have multiple craniofacial anomalies**

We investigated the craniofacial phenotype of *Vax1*$^{-/-}$ embryos from E12.5-17.5 using skeletal preparation and standard histology (n=4 for all stages) (Fig1A-D; E-V, respectively). Consistent with previous reports (Bertuzzi et al. 1999; Hallonet et al. 1999), *Vax1*$^{-/-}$ embryos exhibited lobar HPE associated with narrowing in the maxillary incisor region and SMMCI, but the upper lip remained intact (Appendix Fig. 1). In general, the mutant skull was slightly smaller than WT with obvious retrusion in the maxillary region. The dermatocranium was normal, but multiple defects associated with neurocranial and splanchnocranial elements of the chondrocranium were identified. These predominated along the ventral midline and varied in severity between mutants (Fig. 1D; Ni-iii). Within the nasal cavity, the septum was either hypoplastic or absent, with accompanying hypoplasia of the paraseptal cartilages and vomer. There was CP occurring with complete

penetrance and associated with defects in the paired maxillary and palatine bones. Specifically, a variable circular midline defect affected the body of the pre-maxilla and there was hypoplasia of the palatal shelves. The palatal processes of the maxilla were also hypoplastic and the palatine bone severely disrupted, lacking palatal processes in many cases and exposing the underlying presphenoid bone, which itself lacked medial processes and demonstrated a variable level of hypoplasia within the body, the entire bone being essentially absent in some mutants. The aural and mandibular regions were normal (Appendix Fig. 2).

The CP phenotype was identifiable in all mutants, communicating with the nasal cavity anteriorly and associated with palatal shelves that elevated above the tongue but failed to approximate towards the midline (Figure 1E-V). Gross architecture of the mutant palatal shelves was normal, with no evidence of disrupted growth or development associated with these structures. However, the nasal septum was absent and the nasomaxillary region disrupted by a large midline cavity originating from the forebrain and extending beneath the floor of the hypothalamus (Fig. 1T green asterix). This structure separated the paired VNOs and was demarcated from the oral cavity by only a thin region of neuroectoderm in more posterior regions (Fig. 1U; black arrow). Significantly, paired VNO's were present and situated medially-adjacent to the widened nasal cavity. This suggested that the CP might be secondary to associated defects within the CNS rather than a direct effect of *Vax1* function within the palate.

Vax1 **does not play a direct role in murine palatogenesis**

In order to further understand the role of *Vax1* during palatogenesis we analysed expression in the developing palate from E10.5-14.5 using radioactive *in situ* hybridization. *Vax1* transcripts were identified in bilateral-restricted regions of ectoderm in the medial nasal processes at E10.5, with additional weak expression in midline ectoderm of the fronto-nasal process (n=4) (Fig. 2A-C). The domains of expression within the medial nasal processes persisted during subsequent growth and fusion with the lateral nasal processes

to remain in ectoderm of the presumptive budding vomeronasal organ (VNO) between E11.5-12.5 (n=4 and 6, respectively) (Fig. 2D-F) and ultimately, persist in the VNO itself (data not shown). Significantly, *Vax1* transcripts were not identifiable in either epithelial or mesenchymal regions of the secondary palate from E12.5-14.5 (n=3) (Fig. 2G-J), a finding that was further verified with RT-PCR (Appendix Fig. 3). However, given the failure of the palatal shelves to approximate, we could not definitively rule out a secondary growth defect in the mutant and therefore analysed proliferation in these shelves at E13.5 (Fig. 3A-D). There were no significant differences in epithelial or mesenchymal proliferation indices between WT and *Vax1*$^{-/-}$ at E13.5 or in linear dimensions of the shelves at E14.5 (data not shown). Collectively, these findings suggest that *Vax1* does not play a direct role in development of the secondary palate and that the associated craniofacial defects contributed to the observed CP.

Disrupted proliferation in the early forebrain in the absence of Vax1 function

The evidence to suggest that *Vax1* does not play a direct role in mediating palatogenesis prompted us to investigate gross anatomy of the early craniofacial region in WT and *Vax1*$^{-/-}$ mice at E11.5 (n=4). Interestingly, we found significant truncation in the ventral forebrain region and mid-face of the mutant compared to WT (Fig. 4A-C). We next analysed cell proliferation and apoptosis in this region at the same stage. Consistent with the reduced linear dimensions in these midline regions, we found significantly reduced proliferation in neuroectoderm of the ventral forebrain and mesenchyme within the frontonasal region in the mutant when compared to WT (Fig. 4D-F). However, there were no differences observed in levels of cell death (data not shown).

Reduced Shh signaling in the early craniofacial region in the absence of *Vax1* function

There is evidence that *Vax1* lies downstream of Hedgehog signaling in several developmental models (Hallonet et al. 1999; Kim and Lemke 2006; Take-uchi et al. 2003;

Zhao et al. 2010) and *Vax1* transcripts are directly adjacent to *Shh* in the early ventral forebrain and medial nasal process (Appendix Fig. 4). Given the presence of lobar HPE in *Vax1*$^{-/-}$ embryos associated with abnormal growth in the ventral forebrain and facial midline, we investigated Hedgehog signaling in these regions at E10.5 (n=7 for each group) (Fig. 5A-C, G-I; D-F, J-L). There was evidence of a reduced *Shh* transcriptional domain in the midline ventral forebrain of *Vax1*$^{-/-}$ embryos compared to WT and an accompanying reduction of *Ptch1* in ventral neuroectoderm and facial mesenchyme. We also investigated expression of the direct Shh target *Nkx2.1* (Gulacsi and Anderson 2006; Pabst et al. 2000) and found reduced expression (Fig. 5M-O; P-R). A more quantitative approach was also utilised through qRT-PCR following RNA extraction from dissected E10.5 WT and *Vax1*$^{-/-}$ (n=3 for both groups) embryonic heads (Appendix Fig. 5). mRNA levels of *Shh* and *Ptch1* were significantly reduced in *Vax1* mutants in comparison to WT. Collectively, these data suggest that the craniofacial phenotype associated with loss of *Vax1* function is directly related to reduced Shh signal transduction in the craniofacial region from E10.5.

Loss of *Vax1* function in the absence of *Gas1*

It has been suggested that numerous genetic and environmental factors may influence phenotype in HPE and in some circumstances may be due to mutation in multiple alleles (Ming and Muenke 2002). *Gas1* encodes a Shh co-receptor, with loss of function associated with reduced Shh signaling in the midface and microform HPE (Seppala et al. 2007; Seppala et al. 2014). We therefore investigated the phenotypic consequences of a loss of *Vax1* function in a *Gas1* mutant background. Although the gross craniofacial features of *Gas1; Vax1* compound mutant mice did not differ significantly from individual single mutants, these mice did demonstrate a complete absence of maxillary incisor development (n=4/4), in contrast to single mutants that both have SMMCI (Hallonet et al. 1999; Seppala et al. 2007). Significantly, the midfacial region was normal in the compound

mutants, with paired external nares and an upper lip that remained intact (Appendix Fig. 6).

Discussion

Vax1$^{-/-}$ mice have significant defects in the basal forebrain, including absence of the optic chiasma and preoptic area, medioventral growth defects, pituitary duplication and lobar HPE. There are also facial defects including CP and SMMCI (Bertuzzi et al. 1999; Bharti et al. 2011; Hallonet et al. 1999; Taglialatela et al. 2004), whilst in human populations, *VAX1* is a candidate CLP gene (Butali et al. 2013; de Aquino et al. 2013; de Araujo et al. 2016; Gowans et al. 2016; Peng et al. 2016; Slavotinek et al. 2012; Wang et al. 2016; Wen and Lu 2016; Zawislak et al. 2014) and loss-of-function mutation has been associated with micropthamlmia, optic nerve hypoplasia and absence of the corpus callosum (Slavotinek et al. 2012). We therefore sought to further understand the role of this transcription factor during palatogenesis using the *Vax1*$^{-/-}$ mouse as a model. Significantly, the observed CP appears to be a consequence of the associated gross craniofacial defects, rather than a direct effect of *Vax1* function. There was no evidence of *Vax1* expression in the developing palate and no difference in the gross anatomy or levels of proliferation in the palatal shelves between WT and mutant. It is most likely that a large midline cavity within the CNS, extending from the floor of the hypothalamus through the nasal cavity to the roof of the oral cavity, was responsible for the failure of the palatal shelves to approximate in the midline. This structure has been described previously and ascribed to the presence of CP, but is most likely the cause of this defect (Bertuzzi et al. 1999).

Vax1$^{-/-}$ mice do have lobar HPE and CP is a common feature of this condition, although the precise relationship between these disruptions is poorly understood. In common with other mouse models of HPE (Allen et al. 2007; Cole and Krauss 2003; Martinelli and Fan 2007; Seppala et al. 2007; Tenzen et al. 2006; Zhang et al. 2011; Zhang et al. 2006) *Vax1* mutants have reduced Shh signaling in the early craniofacial midline, consistent with a downsteam role previously identified in other developmental contexts

(Hallonet et al. 1999; Kim and Lemke 2006; Take-uchi et al. 2003; Zhao et al. 2010). However, the reduced *Shh* transcription identified in the ventral forebrain also suggests a requirement for Vax1 in maintaining signaling and an important potential feedback loop in this region. Interestingly, previous investigations have not identified significant differences in *Shh* or *Nkx2.1* expression in the telencephalic neuroectoderm of *Vax1* mutants prior to E12.5 (Bertuzzi et al. 1999). This might be explained by the fact that these changes are subtle; however, we observed them with both *in situ* hybridization and qRT-PCR analysis and the lobar HPE is fully penetrant. The presence of lobar HPE is actually rare in mouse mutants (Geng and Oliver 2009) and with the exception of *Vax1* (Bertuzzi et al. 1999) has only previously been described in mice with loss of Shh co-receptor function (Seppala et al. 2014; Zhang et al. 2011).

In the mouse, *Vax1* is expressed in ectoderm of the medial nasal processes and persists as these structures fuse with the lateral nasal processes at the lambdoid junction during upper lip formation. Moreover, *Vax1* acts as a downstream target of Shh signaling in the medial nasal process, potentially acting to restrict Wnt pathway activity, promote cell cycle exit and epithelial fusion as lip continuity is established (Kurosaka et al. 2014). It is therefore surprising that *Vax1*$^{-/-}$ mice do not display a cleft lip phenotype. One possible explanation is that other factors may compensate for Vax1 function in the early face, particularly during the restriction of Wnt signaling activity in the nasal processes (Kurosaka et al. 2014). Alternatively, thresholds of activity and genetic background may influence phenotypic outcome in the mouse embryo. A closely-related *Vax2* gene exists, but expression is restricted to the developing eye and targeted disruption of both genes results in conversion of the optic nerve to retina, whilst the upper lip remains intact (Mui et al. 2005). Similarly, gross development of the VNO was normal in *Vax1* mutants, despite transcripts being strongly expressed in this organ throughout its development. What is interesting, is that reducing the levels of Shh signal activity in the mid-facial region by generating abrogating *Vax1* on a *Gas1* mutant background did not result in CLP, although the maxillary incisor phenotype did worsen, with agenesis as opposed to SMMCI.

We have investigated the role of *Vax1* during murine craniofacial development and find evidence for reduced Shh signaling in the ventral forebrain associated with reduced levels of proliferation, facial truncation and lobar HPE. Despite expression of *Vax1* in ectoderm of the medial nasal processes the upper lip forms normally in *Vax1* mutant mice. Moreover, the CP would seem to be the result of disrupted craniofacial development rather than a specific function of *Vax1*. In addition, *Vax1; Gas1* mutant mice had a complete absence of the maxillary incisors but upper lip formation remained normal. Despite strong evidence for *VAX1* as a candidate gene for CLP in human populations, this gene is seemingly dispensable for normal upper lip development and plays an indirect role in palatogenesis in the mouse.

Acknowledgements

This work was funded by a Houston Research Fellowship from the European Orthodontic Society awarded to FG. GXM and MS are recipients of National Institute of Health Research UK Clinical Lectureship funded by the Academy of Medical Sciences. The authors declare no potential conflicts of interest with respect to the authorship and/or publication of this research article.

References

Allen BL, Tenzen T, McMahon AP. 2007. The hedgehog-binding proteins gas1 and cdo cooperate to positively regulate shh signaling during mouse development. Genes Dev. 21(10):1244-1257.

Bertuzzi S, Hindges R, Mui SH, O'Leary DD, Lemke G. 1999. The homeodomain protein vax1 is required for axon guidance and major tract formation in the developing forebrain. Genes Dev. 13(23):3092-3105.

Bharti K, Gasper M, Bertuzzi S, Arnheiter H. 2011. Lack of the ventral anterior homeodomain transcription factor vax1 leads to induction of a second pituitary. Development. 138(5):873-878.

Butali A, Suzuki S, Cooper ME, Mansilla AM, Cuenco K, Leslie EJ, Suzuki Y, Niimi T, Yamamoto M, Ayanga G et al. 2013. Replication of genome wide association identified candidate genes confirm the role of common and rare variants in pax7 and vax1 in the etiology of nonsyndromic cl(p). Am J Med Genet A. 161A(5):965-972.

Cole F, Krauss RS. 2003. Microform holoprosencephaly in mice that lack the ig superfamily member cdon. Curr Biol. 13(5):411-415.

de Aquino SN, Messetti AC, Bagordakis E, Martelli-Junior H, Swerts MS, Graner E, Coletta RD. 2013. Polymorphisms in fgf12, vcl, cx43 and vax1 in brazilian patients with nonsyndromic cleft lip with or without cleft palate. BMC Med Genet. 14:53.

de Araujo TK, Secolin R, Felix TM, de Souza LT, Fontes MI, Monlleo IL, de Souza J, Fett-Conte AC, Ribeiro EM, Xavier AC et al. 2016. A multicentric association study between 39 genes and nonsyndromic cleft lip and palate in a brazilian population. J Craniomaxillofac Surg. 44(1):16-20.

Dixon MJ, Marazita ML, Beaty TH, Murray JC. 2011. Cleft lip and palate: Understanding genetic and environmental influences. Nat Rev Genet. 12(3):167-178.

Geng X, Oliver G. 2009. Pathogenesis of holoprosencephaly. J Clin Invest. 119(6):1403-1413.

Gowans LJ, Adeyemo WL, Eshete M, Mossey PA, Busch T, Aregbesola B, Donkor P, Arthur FK, Bello SA, Martinez A et al. 2016. Association studies and direct DNA sequencing implicate genetic susceptibility loci in the etiology of nonsyndromic orofacial clefts in sub-saharan african populations. J Dent Res. 95(11):1245-1256.

Gulacsi A, Anderson SA. 2006. Shh maintains nkx2.1 in the mge by a gli3-independent mechanism. Cereb Cortex. 16 Suppl 1:i89-95.

Hallonet M, Hollemann T, Pieler T, Gruss P. 1999. Vax1, a novel homeobox-containing gene, directs development of the basal forebrain and visual system. Genes Dev. 13(23):3106-3114.

Hallonet M, Hollemann T, Wehr R, Jenkins NA, Copeland NG, Pieler T, Gruss P. 1998. Vax1 is a novel homeobox-containing gene expressed in the developing anterior ventral forebrain. Development. 125(14):2599-2610.

Heyne GW, Everson JL, Ansen-Wilson LJ, Melberg CG, Fink DM, Parins KF, Doroodchi P, Ulschmid CM, Lipinski RJ. 2016. Gli2 gene-environment interactions contribute to the etiological complexity of holoprosencephaly: Evidence from a mouse model. Dis Model Mech. 9(11):1307-1315.

Hong M, Krauss RS. 2012. Cdon mutation and fetal ethanol exposure synergize to produce midline signaling defects and holoprosencephaly spectrum disorders in mice. PLoS Genet. 8(10):e1002999.

Kim JW, Lemke G. 2006. Hedgehog-regulated localization of vax2 controls eye development. Genes Dev. 20(20):2833-2847.

Kurosaka H, Iulianella A, Williams T, Trainor PA. 2014. Disrupting hedgehog and wnt signaling interactions promotes cleft lip pathogenesis. J Clin Invest. 124(4):1660-1671.

Lee CS, May NR, Fan CM. 2001. Transdifferentiation of the ventral retinal pigmented epithelium to neural retina in the growth arrest specific gene 1 mutant. Dev Biol. 236(1):17-29.

Livak KJ, Schmittgen TD. 2001. Analysis of relative gene expression data using real-time quantitative pcr and the 2(-delta delta c(t)) method. Methods. 25(4):402-408.

Martinelli DC, Fan CM. 2007. Gas1 extends the range of hedgehog action by facilitating its signaling. Genes Dev. 21(10):1231-1243.

Ming JE, Muenke M. 2002. Multiple hits during early embryonic development: Digenic diseases and holoprosencephaly. Am J Hum Genet. 71(5):1017-1032.

Mui SH, Kim JW, Lemke G, Bertuzzi S. 2005. Vax genes ventralize the embryonic eye. Genes Dev. 19(10):1249-1259.

Oommen S, Otsuka-Tanaka Y, Imam N, Kawasaki M, Kawasaki K, Jalani-Ghazani F, Anderegg A, Awatramani R, Hindges R, Sharpe PT et al. 2012. Distinct roles of

micrornas in epithelium and mesenchyme during tooth development. Dev Dyn. 241(9):1465-1472.

Pabst O, Herbrand H, Takuma N, Arnold HH. 2000. Nkx2 gene expression in neuroectoderm but not in mesendodermally derived structures depends on sonic hedgehog in mouse embryos. Dev Genes Evol. 210(1):47-50.

Peng HH, Chang NC, Chen KT, Lu JJ, Chang PY, Chang SC, Wu-Chou YH, Chou YT, Phang W, Cheng PJ. 2016. Nonsynonymous variants in myh9 and abca4 are the most frequent risk loci associated with nonsyndromic orofacial cleft in taiwanese population. BMC Med Genet. 17(1):59.

Schambra U. 2008. Prenatal Mouse Brain Atlas, Boston, MA: Springer US.

Seppala M, Depew MJ, Martinelli DC, Fan CM, Sharpe PT, Cobourne MT. 2007. Gas1 is a modifier for holoprosencephaly and genetically interacts with sonic hedgehog. J Clin Invest. 117(6):1575-1584.

Seppala M, Xavier GM, Fan CM, Cobourne MT. 2014. Boc modifies the spectrum of holoprosencephaly in the absence of gas1 function. Biol Open. 3(8):728-740.

Slavotinek AM, Chao R, Vacik T, Yahyavi M, Abouzeid H, Bardakjian T, Schneider A, Shaw G, Sherr EH, Lemke G et al. 2012. Vax1 mutation associated with microphthalmia, corpus callosum agenesis, and orofacial clefting: The first description of a vax1 phenotype in humans. Hum Mutat. 33(2):364-368.

Taglialatela P, Soria JM, Caironi V, Moiana A, Bertuzzi S. 2004. Compromised generation of gabaergic interneurons in the brains of vax1-/- mice. Development. 131(17):4239-4249.

Take-uchi M, Clarke JD, Wilson SW. 2003. Hedgehog signalling maintains the optic stalk-retinal interface through the regulation of vax gene activity. Development. 130(5):955-968.

Tenzen T, Allen BL, Cole F, Kang JS, Krauss RS, McMahon AP. 2006. The cell surface membrane proteins cdo and boc are components and targets of the hedgehog signaling pathway and feedback network in mice. Dev Cell. 10(5):647-656.

Vacik T, Stubbs JL, Lemke G. 2011. A novel mechanism for the transcriptional regulation of wnt signaling in development. Genes Dev. 25(17):1783-1795.

Wang Y, Sun Y, Huang Y, Pan Y, Yin A, Shi B, Du X, Ma L, Lan F, Jiang M et al. 2016. Validation of a genome-wide association study implied that shtin1 may involve in the pathogenesis of nscl/p in chinese population. Sci Rep. 6:38872.

Wen Y, Lu Q. 2016. A clustered multiclass likelihood-ratio ensemble method for family-based association analysis accounting for phenotypic heterogeneity. Genet Epidemiol. 40(6):512-519.

Zawislak A, Wozniak K, Jakubowska A, Lubinski J, Kawala B, Znamirowska-Bajowska A. 2014. Polymorphic variants in vax1 gene (rs7078160) and bmp4 gene (rs762642) and the risk of non-syndromic orofacial clefts in the polish population. Dev Period Med. 18(1):16-22.

Zhang W, Hong M, Bae GU, Kang JS, Krauss RS. 2011. Boc modifies the holoprosencephaly spectrum of cdo mutant mice. Dis Model Mech. 4(3):368-380.

Zhang W, Kang JS, Cole F, Yi MJ, Krauss RS. 2006. Cdo functions at multiple points in the sonic hedgehog pathway, and cdo-deficient mice accurately model human holoprosencephaly. Dev Cell. 10(5):657-665.

Zhao L, Saitsu H, Sun X, Shiota K, Ishibashi M. 2010. Sonic hedgehog is involved in formation of the ventral optic cup by limiting bmp4 expression to the dorsal domain. Mech Dev. 127(1-2):62-72.

Figure legends

Figure 1 Craniofacial phenotypic analysis of WT and *Vax1*$^{-/-}$ mice. (A-D) E17.5 skulls differentially stained for bone and cartilage. (A, B) Lateral (upper panel) and ventral (lower panel) views of WT (A) and *Vax1*$^{-/-}$ (B) skulls demonstrate a smaller size and mid-facial retrognathia associated with the mutant. In addition, the presence of only a single midline maxillary central incisor (red arrow), absence of the nasal septum (green arrow), cleft palate (red *) and fenestrations in the region of the spheno-occipital synchondrosis (yellow arrow) were also identifiable in the mutant when compared to WT (note that the squamosal and frontal bones have been partially removed in the mutant skull). (C, D) Highlight of the ventral maxillary region in WT (C) and mutant skulls (D) demonstrating a spectrum of increasing severity associated with the midline anomalies seen in the mutant (indicated in Di, ii, iii and by the elongated black arrow). In particular, the size of the pre-maxillary midline fenestration (red arrows) and hypoplasia of the palatal processes of the pre-maxilla (orange arrows) and maxilla (pale blue arrows). In addition, the body of the palatine bone was also hypoplastic and lacked palatal processes (dark green arrows), revealing a severe disruption and increasing hypoplasia associated with the pre-sphenoid (violet arrows). Fenestrations were also present in association with the basisphenoid (yellow arrows). (E-V) E12.5-15.5 frontal sections of the anterior, middle and posterior palatal regions stained with Haematoxylin and Eosin. E12.5 WT (E-G) and *Vax1*$^{-/-}$ (H-J) demonstrating constriction of the frontonasal region (black asterix in H) and normal morphology of the palatal shelves in the mutant. E13.5 WT (K-M) and *Vax1*$^{-/-}$ (N-P) demonstrating normal palatal shelf morphology in the mutant. E14.5 WT (Q-S) and *Vax1*$^{-/-}$ (T-V) demonstrating the presence of CP in the mutant and a large midline extension of the CNS within the nasal cavity (green asterix in T) separated from the oral cavity by a layer of neuroectoderm (black arrow in U).

Glossary for Fig. 2 and Appendix Fig. 1. **ab**, alveolar bone of mandible; **agp**, angular process of mandible; **als**, alisphenoid; **bb**, basal bone of mandible; **bo**, basioccipital; **bps**, body of preshenoid; **bs**, basisphenoid; **cbi**, crus brevis of incus; **cdp**, condylar process of mandible; **cli**, crus longus of incus; **cna,** cupola nasi anterior; **crp**, coronoid process of mandible; **c1**, first cervical vertebra; **eo**, exoccipital; **fpmx**, frontal process of maxilla; **fr**, frontal; **go**, gonial; **in**, incus; **ip**, interparietal; **jg**, jugal; **li**, lower incisor; **lo**, lamina obturans; **ma**, mandible; **MC**, Meckel's cartilage; **mm**, manubrium of malleus; **mpps**, medial process of presphenoid; **mx**, maxilla; **na**, nasal; **ns**, nasal septum; **pbm**, processus brevis of malleus; **pca**, pars canalicularis; **pco**, pars cochlearis; **pl**, palatine; **plpps**, posterior lateral process of presphenoid; **pmx**, premaxilla; **ppmx**, palatine process of maxilla; **pppl**, palatine process of palatine; **pppx**, palatal process of premaxilla; **pr**, parietal; **ps**, preshenoid; **ptg**, pterygoid; **so**, supraoccipital; **sp**, styloid process; **sq**, squamosal; **st**, stapes; **tr**, tympanic ring; **ui**, upper incisor; **vo**, vomer; **zpsq**, zygomatic process squamosal.

Figure 2 Expression of *Vax1* in the early facial region. (A-H) 35^S radioactive *in situ* hybridization on frontal sections through the developing facial region. (A-C) E10.5. (D, E) E11.5. (F) E12. (G-J) Digoxigenin-labelled *in situ* hybridization through the developing palatal shelves. (G) E12.5; (H, I) E13.5 frontal and sagittal, respectively; (J) E14.5.

Figure 3 Cell proliferation in the developing palatal shelves at E13.5. (A–B) BrdU analysis of E13.5 (A) WT and (B) *Vax1*$^{-/-}$ palatal shelves. BrdU-positive cells were counted in the mesenchyme and epithelium of the middle palatal shelf. For mesenchyme, counting was undertaken within an ocular scale grid (black box) orientated at the apex (lower box: 0.03 mm^2) and bend (upper box: 0.015 mm^2) regions. For epithelium, counting was undertaken within 263 μm and 165 μm lengths of epithelium at the palatal apex (lower dotted line) and bend (upper dotted line), respectively. (C, D) Percentage BrdU incorporation for (C) epithelium and (D) mesenchyme. A total of 3 WT and 3 *Vax1*$^{-/-}$ mice

were analysed. Student's *t* tests were performed to assesses whether the means between groups were statistically different from each other. Data is represented as mean and standard deviation. *P* values of less than 0.05 were considered statistically significant. Proliferation rates were not statistically different for either region.

Figure 4 Reduced growth in the ventral forebrain and frontonasal region of *Vax1*$^{-/-}$ mice. (A, B) Linear dimensions of E11.5 WT (A) and *Vax1*$^{-/-}$ (B) embryos at the craniofacial midline. Lines were constructed from most anterior point of the isthmus [1] to the hypothalamus [2]; from [1] to the most anterior point of the septum [3]; from [3] to the optic recess [4] and from [4] to the most anterior-superior point at the fronto-nasal region [5]. (C) Statistical analysis showing a significant difference in linear dimensions between WT and mutant embryos for all constructed distances. (D, E) BrdU labelling of E10.5 WT (D) and *Vax1*$^{-/-}$ (E) embryos at the craniofacial midline. Percentage positive cells were calculated within (0.012 mm^2) scale grids at the [1]=septum; [2]=median ganglionic eminence; [3]=median eminence; [4]=hypothalamus and [5]=facial mesenchyme. (F) Statistical analysis showing a significant difference in percentage proliferating cells between WT and mutant embryos at all locations measured. A total of 3 WT and 3 *Vax1*$^{-/-}$ mice were analyzed. Student's *t* tests were performed to assesses whether the means between groups were statistically different from each other. *P* values of less than 0.05 were considered statistically significant. Data is represented as mean and standard deviation (*P<0.05; **P<0.001).

Figure 5 Disrupted Shh signaling in the early forebrain of *Vax1*$^{-/-}$ embryos. (A-H) 35^S radioactive *in situ* hybridization on E10.5 sagittal sections through the developing craniofacial region of WT (A-C; G-I; M-O; S-U) and *Vax1*$^{-/-}$ (D-F; J-L; P-R; V-X) embryos. (A-F) *Shh*. (G-L) *Ptch1*. (M-R) *Nkx2.1*.

Figure 1

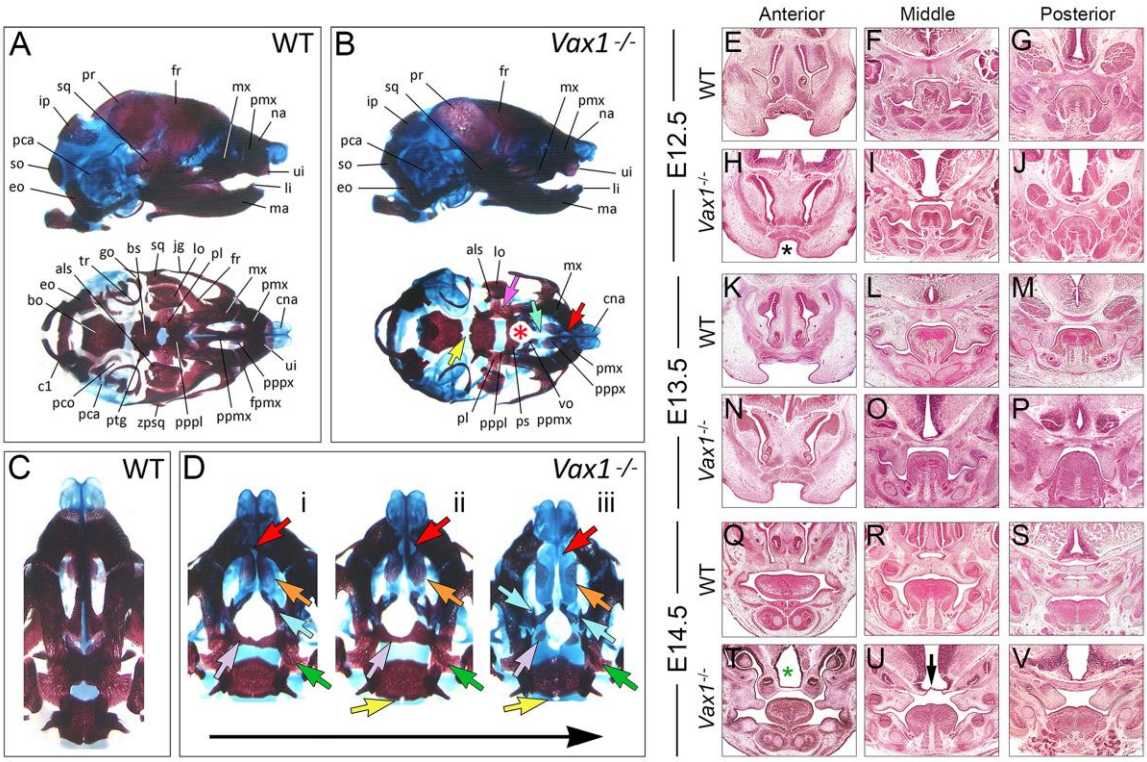

Figure 2

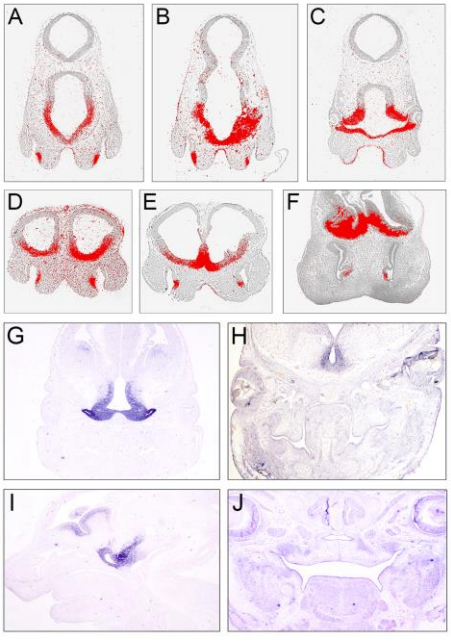

3

Figure 3

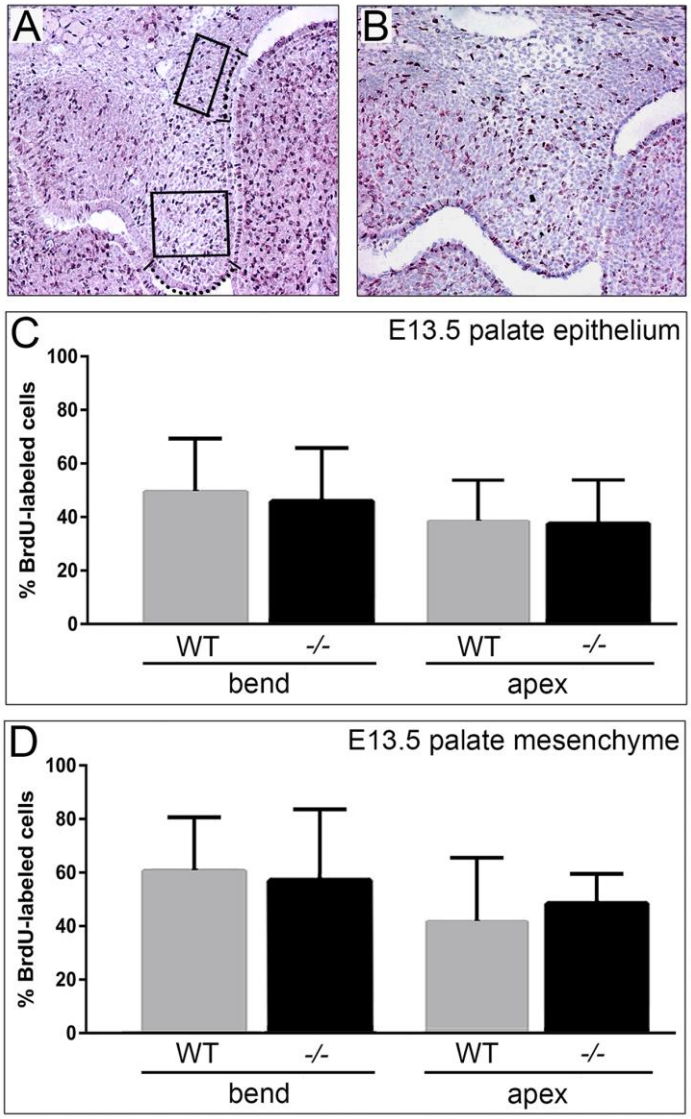
A
B
C
E13.5 palate epithelium
% BrdU-labeled cells
100
80
60
40
20
0
WT
-/-
WT
-/-
bend
apex
D
E13.5 palate mesenchyme
% BrdU-labeled cells
100
80
60
40
20
0
WT
-/-
WT
-/-
bend
apex

Figure 4

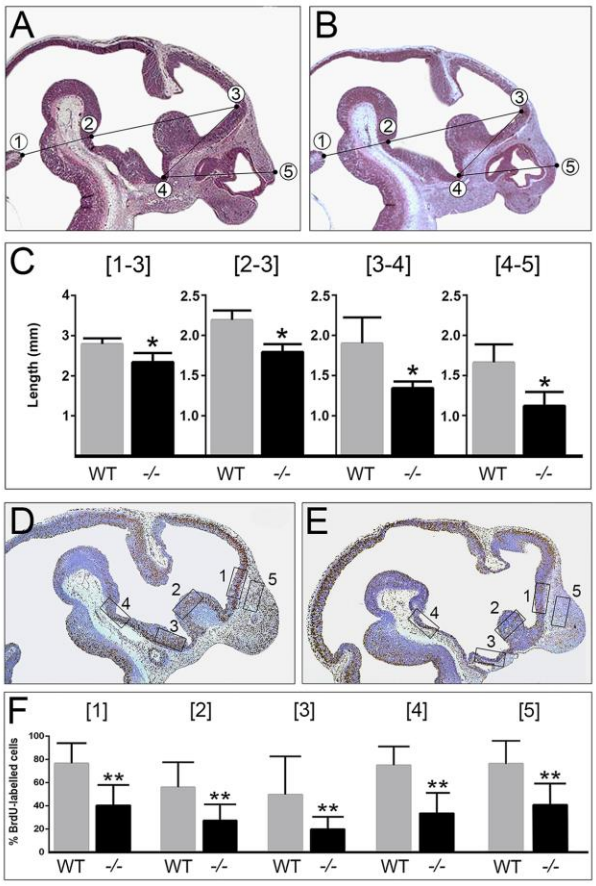

Figure 5

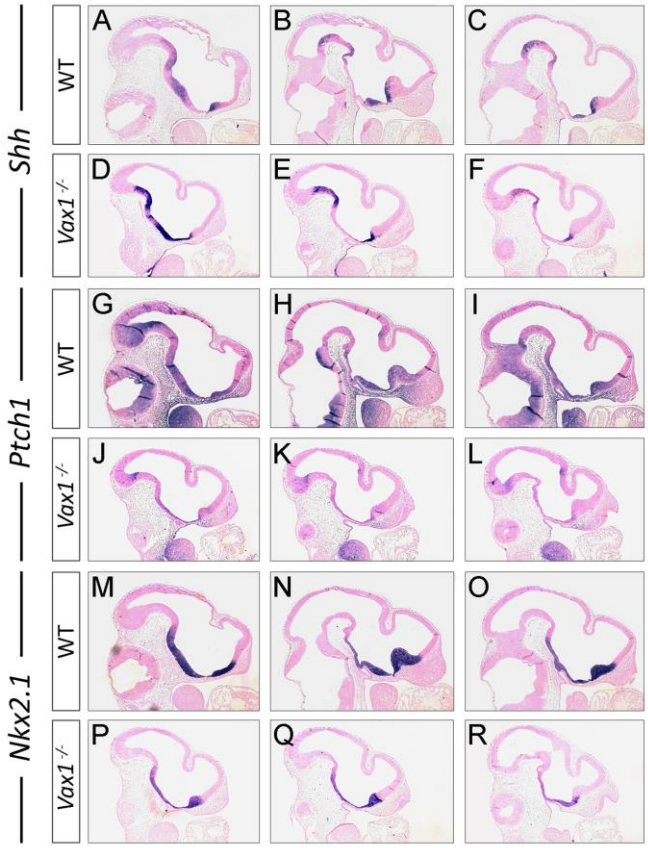

Appendix material

Appendix Figure 1 Histological analysis of the craniofacial midline at E12.5 and E15.5. (A, B) At E12.5, *Vax1*$^{-/-}$ mice have lobar HPE associated with narrowing of the anterior maxillary region and SMMCI (red arrow), but the upper lip remains intact. (C, D) At E15.5, in more posterior regions of the oral cavity, a duplicated pituitary gland was seen in the mutant extending through the cranial base into the oral cavity (green arrow) (Bharti et al. 2011). At E16.5, in the CNS there is fusion of the lateral ventricles and absence of the septum (s).

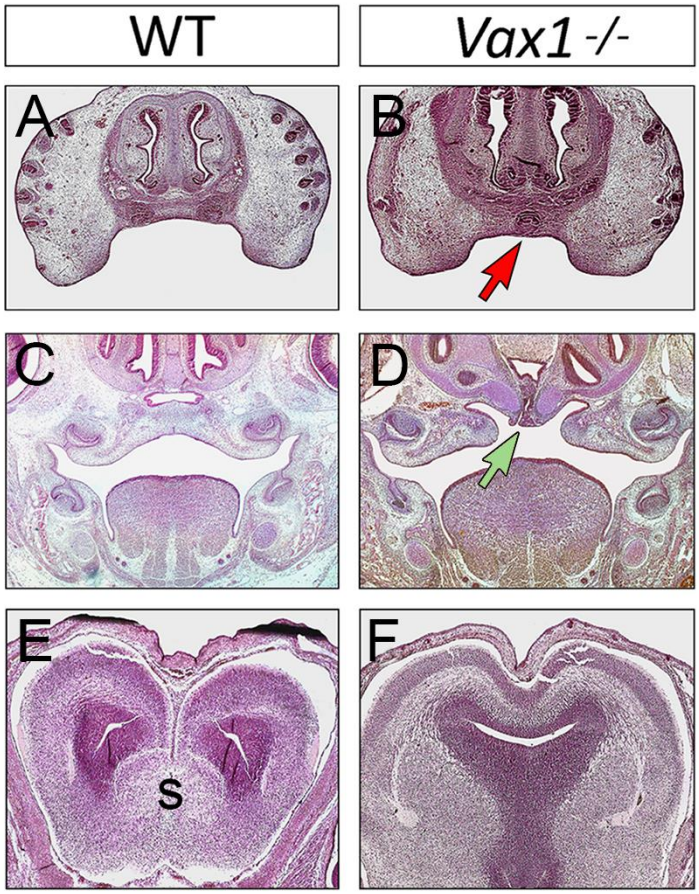

Appendix Figure 2 Skeletal preparation of the developing skull at E17.5. (A, B) Ventro-lateral highlight of the developing palate (anterior is to the right) in (A) WT and (B) *Vax1*$^{-/-}$. Note an absence of the nasal septum and hypoplasia of the vomer in the mutant. (C, D) Highlight of the ventral pre-sphenoid in (C) WT and (D) *Vax1*$^{-/-}$, showing an absence of the medial process (purple arrowhead) and hypoplasia of the body (violet arrowhead). (E, F; G, H) Comparison of WT middle ear and mandibular skeletal elements, respectively. No defects in the gross anatomy of these regions could be identified, although the mutant mandible was a little smaller. For full glossary see Figure 1 legend.

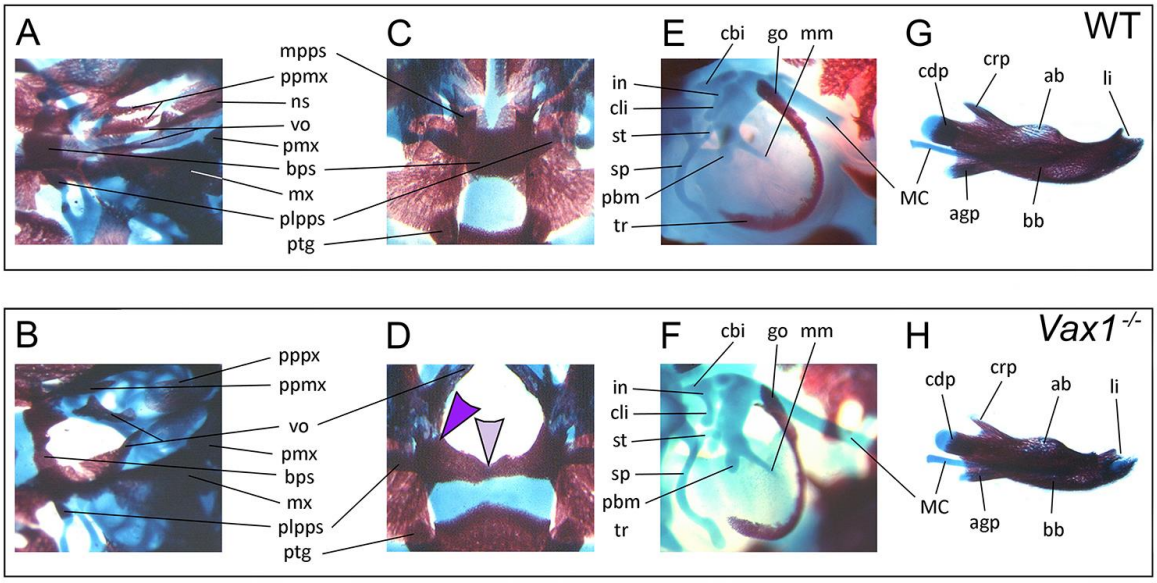

Appendix Figure 3 RT PCR analysis of *Vax1* expression in the frontonasal process and palatal shelves. (A) Gel electrophoresis of PCR products derived from RT-PCR analysis of *Vax1* (lanes 2-5) and *β-actin* (8-11) expression in craniofacial tissues. (2) E12.5 and (3) E14.5 frontonasal process; (4) E12.5 and (5) E14.5 palatal shelves; (8) E12.5 and (9) E14.5 frontonasal process; (10) E12.5 and (11) E14.5 palatal shelves. Line (6) is the negative control and line (12) the positive control (total murine RNA at E12.5). The *Vax1* band has 200 base pairs and the *β-actin* band 100 base pairs. (1 and 7) 100 base pair marker.

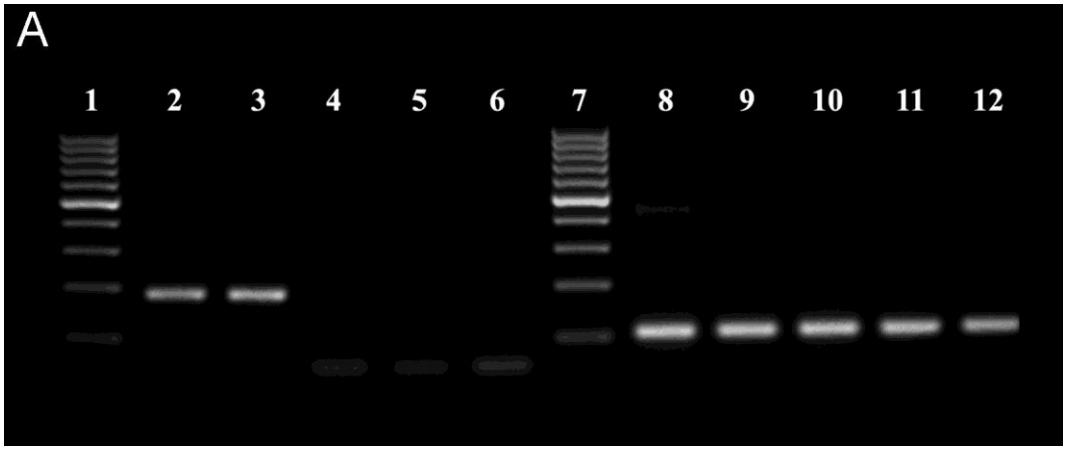

RNA was isolated from the frontonasal process and palatal shelves of E12.5 and E14.5 WT and *Vax1*$^{-/-}$ embryos using a RNeasy RNA Purification Kit (Qiagen) according to the manufacturer protocol. RNA was reverse transcribed and the cDNA used as a template for PCR. *β-actin* was used as a reference gene. The following primer oligonucleotides were used:

Vax1 F 5'CAAGGAGAGCCGGGAGATCAAG

Vax1 R 5'TTCTCGGATAGACCCCTTGGC

RT-PCR Steps	Temperature	Time	Number of cycles
Synthesize 1st Strand DNA	48 °C	45 minutes	1
Denature template	94 °C	2 minutes	1
Denaturation	94 °C	30 seconds	35
Anealling	58 °C	1 minute	35
Extension	68 °C	2 minutes	35
	68 °C	7 minutes	1
	4 °C	forever	forever

Appendix Figure 4 *Shh* and *Vax1* expression in the craniofacial midline. (A-D) E11.5 sagittal sections through the developing craniofacial region showing adjacent expression of (A, C) *Vax1* and (B, D) *Shh* in neuroectoderm of the ventral forebrain and ectoderm of the medial nasal process.

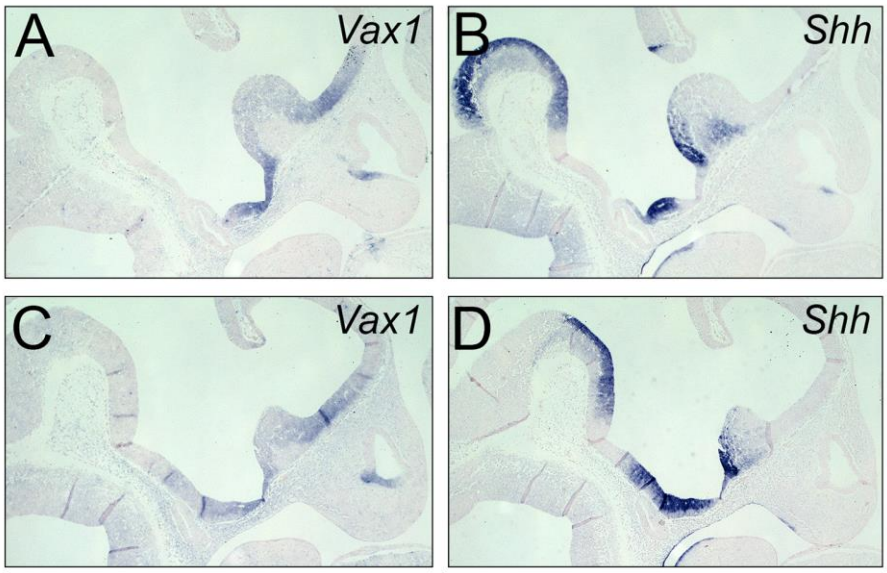

Appendix Figure 5 qRT-PCR analysis of Shh signaling activity in embryonic heads at E10.5. (A, B) Expression of (A) *Shh* and (B) *Ptch1* in WT and *Vax1*$^{-/-}$ heads (n=3+3, respectively). Students' t-tests were utilized to analyse the relative levels of expression of *Shh* and *Ptch1* in both WT and mutant tissue normalized relative (per copy) to the housekeeping gene ***β-Actin*** (Livak and Schmittgen, 2001).

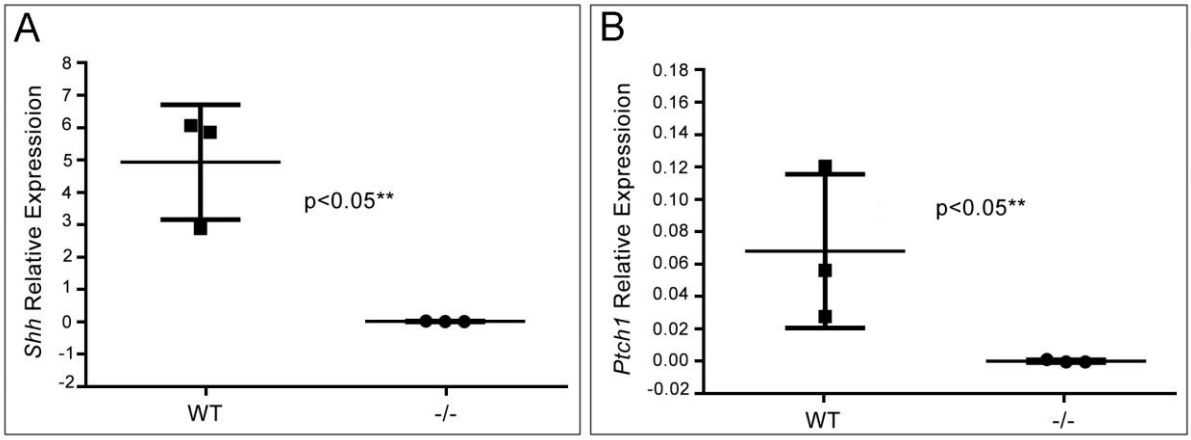

Appendix Figure 6 ***Vax1; Gas1*** **compound mutant mice.** (A-C) E15.5 gross appearance of the midface. (D-F) E15.5 frontal sections through the developing maxillary incisor region stained with Haematoxylin and Eosin. (A, D) WT. (B, E) *Vax$^{-/-}$; Gas1$^{+/+}$.* (C, F) *Vax$^{-/-}$; Gas$^{-/-}$.* There is a gradation of maxillary incisor phenotype in Gas1; Vax1 compound mutant mice. In WT mice two maxillary incisor teeth are present in the craniofacial midline (D, arrowed), whilst *Vax$^{-/-}$; Gas1$^{+/+}$* mice have SMMCI (E, black circle) and *Vax$^{-/-}$; Gas$^{-/-}$* mice have a complete absence of maxillary incisors (F, black asterix). Note the presence of bilateral nares and an intact upper lip in all mice (A-C).